

The systematical actions of Resveratrol against Nasopharyngeal Carcinoma Based on Network Target Prediction and Experimental Verification

Bo Zhou

Dalian Medical University

Zihan Xu

Dalian Medical University

Tengjun Man

Dalian Medical University

Yujuan Yi

Dalian Medical University

Hong Tang

The First Affiliated Hospital of Dalian Medical University

Jia Li

The First Affiliated Hospital of Dalian Medical University

Zheng Sun (✉ sunclank@163.com)

Dalian Medical University

Research Article

Keywords: Nasopharyngeal Carcinoma, Resveratrol, Network Target Prediction, anti-Proliferation, Apoptosis, MAPK signaling pathway

Posted Date: March 29th, 2022

DOI: <https://doi.org/10.21203/rs.3.rs-1414226/v1>

License:   This work is licensed under a Creative Commons Attribution 4.0 International License.

[Read Full License](#)

Abstract

In this study, we aimed to find the targets of resveratrol in nasopharyngeal carcinoma (NPC) by network target prediction and investigate the possible mechanisms through experimental verification. Firstly, resveratrol and NPC-specific targets were combined with protein-protein interactions to construct a systematical resveratrol targets-NPC network. Consistently, molecular docking was performed to predict the molecular determinants of resveratrol against NPC. In order to clarify this point, the anti-cancer effects of resveratrol were investigated in the CNE2 cell lines in vitro and NPC cases in vivo. Functional enrichment results suggested that resveratrol played anti-NPC role mainly through MAPK pathway and the potential targets were MAPK1, MAPK3, STAT3, TP53, PIK3CA, PIK3R1, SRC, MAPK8, RELA and VEGFA. In vitro, resveratrol inhibited proliferation, invasion, migration and eventually induced apoptosis in CNE2 cells on time-and dose-dependent manner. Meanwhile, western blot confirmed that resveratrol exerted apoptotic activity of NPC cells by inhibiting MAPK cell signaling activation. Clinically, Immuno-histochemical staining showed significant differential p-ERK1/2, p-JNK and p-P38 activation between tumor-surrounding and NPC cases. Altogether, our findings identified resveratrol could play potent inhibition and apoptosis on human NPC cells possibly by targeting MAPK pathways and suggested that resveratrol had the potential to be an effective bioactive compound in NPC patients.

Introduction

As an epithelial disease occurring in the nasopharyngeal mucosal^{1,2}, nasopharyngeal carcinoma (NPC) is one of the most widely recognized malignancies of the head and neck, which is distributed in surprisingly different geographic regions covering a wide variety of races³. It is highly prevalent in southern China, where the incidence is 20 to 50 cases per 100,000 males⁴. The cause of NPC is multifactorial⁵ and closely associated with host genetics, EBV infection⁶, active and passive tobacco smoking, consumption of preserved foods and alcohol⁷. Nowadays, the most common treatment of NPC is the use of combination of surgical resection, radiotherapy, and chemotherapy, which greatly increase the survival rate of NPC patients⁸. Be that as it may, on account of counteractive chemotherapy drug effect, authentic side effect can be delivered by consolidated treatment, which will be the bringer of the inappropriate treatment⁹. Similarly, distant metastasis is an important cause of treatment failure^{10,11}. For these reasons, the search for the NPC drugs with high efficiency and low side effect has gradually turned into a research area clinically.

Resveratrol (trans-3,4',5-trihydroxystilbene, Res) has been existing in many kinds of plants, and among these plants, *Polygonum cuspidatum* Siebold & Zucc is the richest source for resveratrol production. Its root is widely used as a traditional medicine cultivated in Asian countries to treat hyperlipidemia, trauma, and inflammatory diseases^{12,13}. Such miscellaneous pharmacological properties as antioxidant, anti-aging, anti-inflammatory, anti-cancer, anti-diabetes, cardiac safety and neuro insurance does resveratrol have^{14,15}. Recently, resveratrol has been reported to anti-proliferation and anti-apoptosis induction of

nasopharyngeal carcinoma cells¹⁶⁻¹⁸. Nevertheless, the molecular mechanism of its function has a long way to go in terms of methodological study.

With the principles of system biology, network pharmacology is used for the explanation of the development of diseases from the holistic perspective of network equilibrium. This approach helps to understand the link between drugs and disease and is characterized by "multi-quality, multi-target" approached¹⁹⁻²¹. In that light, this is a potential direction for research that could systematically look at NPC targets of resveratrol by means of various database resources²². In our case, the pharmacokinetic (PK) parameters of resveratrol were gathered in the first place from TCMSP server. After that, a Potential Candidate Target for Resveratrol and a Therapeutic Target Gene for NPC were acquired from extensive databases respectively. In addition, the predication and construction for the potential candidate target genes were made using online pharmacology databases. Furthermore, enrichment of the Gene Ontology (GO) function analysis and Kyoto Encyclopedia of Genes and Genomes (KEGG) pathway were assessed using STRING and Metascape online database. Molecular docking was then used to determine the mutual effect happened between resveratrol and key targets. Finally, the essential targets and pathways of resveratrol against NPC were validated by in vitro and in vivo experiments such as NPC cells sensitivity detection, proliferation analysis, apoptotic fluorescence staining, western blot, and immunochemistry staining. Graphical abstract was in Fig. 1.

Materials And Methods

1. Network Pharmacology Analysis

1.1 Collection of PK Parameters

PK parameters of resveratrol were procured from TCMSP data set rendition (<http://tcmsp.com/tcmsp.php>)²³, which included 499 Chinese spices enrolled in the Chinese Pharmacopeia and 29,384 ingredients²⁴. In addition, data on its absorption, distribution, metabolism and excretion properties can be obtained.

1.2 Resveratrol Targets

Resveratrol targets were acquired from databases and literature. Firstly, its three-dimensional structure was obtained from PubChem as shown in Fig. 2A (<https://pubchem.ncbi.nlm.nih.gov/>)²⁵. Then, the targets of resveratrol were collected from the SwissTargetPrediction (<http://www.swisstargetprediction.ch>)²⁶, DrugBank (<http://www.drugbank.ca>)²⁷, Traditional Chinese Medicine Systems Pharmacology Database and Analysis Platform, PharmMapper (<http://www.lilabecust.cn/pharmmapper/>)^{28,29}. Acquired targets were then mapped to the UniProt database (<http://www.uniprot.org/>)³⁰ for normalization.

1.3 Identification of NPC Targets

The DisGeNET platform (<http://www.disgenet.org>)³¹, GeneCards (<https://www.genecards.org>)³², TTD (<http://bidd.nus.edu.sg/group/cjttd>)³³, OMIM (<http://www.omim.org>)³⁴ and the Comparative Toxicogenomics Database (<http://ctdbase.org/>)³⁵ were selected to collect NPC genes by searching words “nasopharyngeal carcinoma” and reproducible targets were removed.

1.4 Construction of Protein-Protein Interaction (PPI) Data

Intersecting targets for nasopharyngeal carcinoma and resveratrol were obtained using Venny 2.1.0 (<http://bioinfogp.cnb.csic.es/tools/venny/index.html>) and the overlapping targets were then uploaded to the STRING 11.0 (<https://string-db.org/>). The pharmacology network that made up the hubs of the networks were resveratrol, NPC, and their connected target genes.

1.5 Analysis of GO Function Enrichment and KEGG Pathway

Useful pathways of resveratrol connected with NPC were dissected with GO enrichment and KEGG pathways analysis. The GO incorporated a biological process (BP), molecular function (MF), and cellular component (CC). The Component-target-disease-pathway interaction network was constructed by Cytoscape version 3.8.2, which was a java based open-source software³⁶. The enrichment degree of P-value < 0.05 was considered statistically significant.

2. Application of Ligand-protein Molecular Docking

Receptor ligand atomic docking was utilized to survey the cooperation among resveratrol and its protein targets including MAPK1(6slg), MAPK3(4qtb), STAT3(2xa4), TP53(5mhc), PIK3CA(4jps), PIK3R1(5gji), SRC(4mxo), MAPK8(4ux9), RELA(3qxy) and VEGFA(3qtk). The key structures were gotten from Protein Data Bank (<http://www.rcsb.org/>)³⁷. The resveratrol MOL2 design document was downloaded from the TCMSp database. The molecular docking results were generated by running autogrid4 and autodock4. A partial plot of the molecular docking was obtained using PyMol software.

3. Experiments Verification

3.1 Reagents

Resveratrol purchased from Solarbio (Solarbio, Beijing) was dissolved at a stock concentration of 50 mmol/L in dimethyl sulfoxide (DMSO) and the final DMSO concentration was not exceeding 0.1%.

3.2 Cell Culture and Treatment

A poorly differentiated human NPC cell line (American Type Culture Collection, ATCC)^{38,39} was cultured in RPMI-1640 medium (Gibco, USA) supplemented with 10% fetal bovine serum (FBS; Gibco). All cells were incubated at the temperature of 37°C with 5% CO₂.

3.3 Cell Proliferation Assay

The effect of resveratrol on the cell growth of CNE2 cells was examined using the Cell Counting Kit-8 (CCK-8) assay (Abbkine, USA). NPC cells were plated in 96-well plates at 5,000 cells/well. Cells incubated in 96-well plates were treated as indicated and cell proliferation was assessed by CCK-8 assay at 0, 24, 48 and 72-hour resveratrol treatment following the manufacturer's instruction. Viable counts were determined with absorbance readings at 450 nm by a SpectraMax M5 plate-reader (Molecular Devices, Sunnyvale, CA, USA) and IC50 were calculated on GraphPad Prism 8.

3.4 Hematoxylin-eosin (H&E) Staining

CNE2 cells were treated with 50 and 100 μ M resveratrol and washed with PBS. Then, the cells were immobilized over night with 4% paraformaldehyde and stained with H&E. The stained sections were imaged under an inverted phase contrast microscope (Nikon, Japan).

3.5 Terminal Deoxynucleotidyl Transferase dUTP Nick-End Labeling (TUNEL) staining

The Apoptosis of NPC was detected by TUNEL staining. According to the manufacturer's instructions, the apoptosis cells were detected by TUNEL assay Kit (Alexa Fluor 640, Yeasen, China). Nuclei counterstained with DAPI staining and viewed 400x under inverted microscope (Leica DM400DB microscope, Germany). The rate of apoptosis was measured by the number of normal positive cells (red spot) in the fluorescent picture.

3.6 Wound Scratch Assay

NPC cells were cultured in 24-well plates with 5×10^4 cells/well and incubated at 37°C with a 5% CO₂ incubator. The cell monolayer was scraped in a straight line to create a scratch with a 1 mL pipette tip, and the debris was removed by washing the cells with PBS. Scratches were observed under a microscope (Nikon, Japan) at 24 and 48-hour. The results of the scratches represented the mean of the three experiments.

3.7 Transwell Migration Assay

In the migration assay, the cells were digested and suspended in serum-free medium. A total of 100 μ L of cell suspension (5×10^4) was added to the upper chamber of the transwell plate and 500 μ L of medium containing 10% FBS was added to the bottom chamber. After incubation at 37°C and 5% CO₂ for 48 hours, the cells were gently removed from the upper surface of the polycarbonate film with a damp cotton swab. The polycarbonate film was carefully removed from the upper chamber and the cells were immobilized in precooled methanol for 30 minutes. After staining with 0.1% crystal violet for 20 minutes, the specimens were observed under microscope (Nikon, Japan) and photographed.

3.8 Western Blot Analysis

After treating NPC cells with resveratrol, whole Lysis were harvested, and Western blotting was performed to detect target proteins. MAPK Family Antibody Sampler Kit ERK1/2, JNK, P38 (1:1000; 9926; CST; USA)

and Phospho-MAPK Family Antibody Sampler Kit p-ERK1/2, p-JNK, p-P38 (1:1000; 9910; CST; USA) were used. β -actin antibody was purchased from Abclonal (1:50000, a00702, Abclonal, MA, USA). The total protein was obtained by tissue lysis and its concentration was measured. The protein separated by PAGE was moved to PVDF film and added with primary and secondary antibodies. Then, the protein was exposed, developed and fixed on x-ray film with ECL chemiluminescent reagent.

3.9 Immunohistochemical (IHC) staining of NPC Human Tissues

IHC staining was conducted with 36 NPC surgical specimens and, where possible, their noncancerous counterparts. The p-ERK1/2 (1:500), p-JNK (1:50), and p-P38 antibodies (1:200) were selected because of the network target prediction. The sections without first antibody incubation were used as background control. IHC staining was observed and shot with magnifying lens. Spot staining power was examined utilizing Image Pro Plus 6.0 programming (Rockville, USA) and addressed by the mean optical density value.

3.10 Statistical Analysis

Measurement data were expressed by mean \pm standard deviation (SD). Statistical significance between different groups was determined by one-way-ANOVA analysis using GraphPad Prism 8.3.0 (GraphPad Software Inc., San Diego, CA, USA), and $P < 0.05$ (two tails) was considered statistically significant.

3.11 Ethics approval and consent to participate

In accordance with approval from the ethics committee of First Affiliated Hospital of Dalian Medical University (NO. PJ-KS-KY-2022-26), all participants signed an informed consent before enrolled in this research. The stages of this study were performed based on the ethical principles in the Helsinki Declaration.

3.12 Consent for publication

The authors appreciate all the patients in this work for their cooperation and permission for the publication of the article.

Results

4.1 Network Pharmacology Analysis

4.1.1 PK Parameters

The data of resveratrol on 12 primary characteristics like Caco-2 and BBB for drug screening were assessed (Table 1). It is noteworthy that OB is a key feature of orally administered drugs, as it plays a crucial role in assessing the effectiveness of drug distribution in the body cycle. Despite the low

bioavailability of resveratrol, resveratrol has a therapeutic effect on NPC. It is also worth noting that the relatively small molecular weight of resveratrol allows it to cross the blood-brain barrier.

Table 1
Pharmacological and molecular properties of resveratrol

MW	Alog P	Hdon	Hacc	OB (%)	Caco-2	BBB	DL	FASA-	TPSA	RBN	HL
228.26	3.01	3	3	19.07	0.80	-0.01	0.11	60.69	0.49	2	0.00

4.1.2 Potential Target Genes and Network Analysis

2817 NPC-related genes (Supplementary Table 1) and 402 drug target genes (Supplementary Table 2) were screened through Venny 2.1.0 mapping to screen out 223 overlapping targets (Fig. 2B).

4.1.3 PPI Networks

The 223 targets were input into the STRING platform to obtain PPI network maps (Fig. 2C). High degree, betweenness, and closeness target genes were selected as hub genes in NPC (Supplementary Table 3). Then, the predicted mode of 10 hub genes included MAPK1, MAPK3, STAT3, TP53, PIK3CA, PIK3R1, SRC, MAPK8, RELA and VEGFA. In the above 10 hub proteins, MAPK1, MAPK3 and MAPK8 were involved in apoptotic pathways (Fig. 2D).

4.1.4 GO Enrichment and Pathway Analysis

To clarify the capacity and pharmacological instrument of resveratrol, we conducted GO enrichment and KEGG pathway analysis (Supplementary Table 4) of the 223 targets. GO analysis focuses on biological process (BP), cell component (CC), and molecular function (MF) items. GO enriched the top ten entries in BP, CC and MF (Fig. 3A). Particularly, the enriched BP ontologies were overwhelmed by response to inorganic substance, response to wounding and positive regulation of cell death, etc. The enriched MF ontologies were overwhelmed by kinase activity, kinase binding and so on. Among them, CC analysis accounted for the largest proportion of membrane rafts (30 target genes). Then, a sum of 20 critical pathways were obtained ($P < 0.05$) and were showed in Fig. 3B. A network diagram of "Component-target-disease-pathway" interaction was made by Cytoscape software (Fig. 3C). Therefore, the MAPK signaling pathway may be the pathway for its role in the treatment of NPC (Fig. 3D).

Table 2
Binding energy and related sites of resveratrol to key proteins

Target (PDB ID)	Drug	Binding sites	Docking score
MAPK1 (6slg)		LEU-294, ASN-297, ASP-251, LYS-272,	-6.12
MAPK3 (4qtb)		ASN-271, SER-246	-5.63
STAT3 (2xa4)		ASP-123, VAL-100, HIS-97, ARG-370	-5.21
TP53 (5mhc)		HIS-907, VAL-911, LYS-912	-6.54
PIK3CA (4jps)	Resveratrol	GLU-86, GLU-91	-5.55
PIK3R1 (5gji)		CYS-844, ILE-633, GLY-842, HIS-676	-6.54
SRC (4mxo)		ASP-367, ALA-360, LYS-363	-5.43
MAPK8 (4ux9)		ARG-500, GLU-504, GLU-505	-5.38
RELA(3qxy)		LYS-222, ILE-223, GLN-240	-5.38
VEGFA (3qtk)		GLU-132, ARG-139, ASP-201, SER-399, ASN-404	-5.17

4.1.5 Molecular Docking Analysis

The results uncovered that docking scores of resveratrol with hub target went from - 5.17 to -6.54. Particularly, the docking results of resveratrol with MAPK1, MAPK3 and MAPK8 revealed that resveratrol was situated in the limiting site of the hub target. As shown in Fig. 4 and Table 2, other central proteins also showed better affinity for resveratrol.

4.3 Experimental Verification

4.3.1 Resveratrol Reduced the Viability of CNE2 Cells

CNE2 cells were treated with increasing concentrations of resveratrol for 24, 48, 72-hour, followed by Cell Counting Kit-8 (CCK-8) assay. Compared to that of control groups, the cell viability was significantly decreased by resveratrol treatment in a dose-dependent manner and the IC₅₀ of resveratrol on CNE2 at 24h, 48 h and 72h was 99.13, 77.78 and 79.34 $\mu\text{mol/L}$, respectively (Fig. 5A). Then, the resveratrol-sensitivity of NPC cells was tested by HE staining. As shown in Fig. 5B, CNE2 cells presented spindle-shaped and segments of cell bodies after 50 and 100 μM resveratrol treatment for 24-hour and 48-hour. In brief, resveratrol treatment reduced the cellular activity of NPC cells at different time and dosage points.

4.3.2 Resveratrol Induced Apoptosis in CNE2 Cells

TUNEL staining was performed to estimate the effect of resveratrol on apoptosis in CNE2 cells. After being treated with Resveratrol (50 and 100 μ mol/L) for 48 hours, the apoptotic cells significantly increased under different resveratrol concentration compared with control groups (Fig. 5C, D).

4.3.3 Resveratrol Inhibits Invasion and Migration of CNE2 Cells

Considering the correlation between resveratrol and metastasis of NPC, the migration and invasiveness of resveratrol in NPC cells were tested by cell migration and invasiveness assay. Firstly, CNE2 cells were treated with resveratrol for 24-hour and 48-hour. Through the experiment of wound healing, the migration index of CNE2 cells was higher in the control group (Fig. 6A, B). Meanwhile, we also studied the invasiveness ability of CNE2 cells (Fig. 6C). The invasiveness of CNE2 cells decreased with the increase of time and drug concentration (Fig. 6D). These data suggested that resveratrol resulted in repressed migration and invasiveness of NPC cells.

4.3.4 Regulation of MAPK Pathway in Resveratrol Treated CNE2 Cells

To test the speculation of resveratrol target mitogen-activated protein kinase (MAPK) family members in CNE2 cells, we examined the expression of three MAPK pathway-related proteins ERK1/2, P38 and JNK and their phosphorylated proteins by Western blot. As shown in Fig. 7, the ratio of p-ERK1/2 to ERK1/2 had no significant difference between the control group and the 50 μ M treated group, but there was significant difference between the 100 μ M treated group ($P < 0.001$). Moreover, the ratio of p-P38/P38 and p-JNK/JNK was significantly decreased after 24-hour resveratrol treatment, and the effect was more significant after 48-hour treatment. These results suggested that resveratrol mediated the inactivated role of MAPK signaling pathway in NPC cells.

4.3.5 Differential MAPK Expression Patterns of NPC

To analyze the clinical significance of MAPK pathway, we studied the expression in NPC tissues using immunohistochemical staining. The expression pattern of p-ERK1/2, p-P38 and p-JNK were analyzed, and the results demonstrated that the NPC group had significantly higher p-ERK1/2, p-P38 and p-JNK expression than that in the surrounding noncancerous counterparts (Fig. 8). IHC staining results indicated that MAPK signaling pathway was specifically activated in NPC patients.

Discussion And Conclusion

Nasopharyngeal carcinoma (NPC) is a highly invasive epithelial malignancy arising from nasopharyngeal mucosal lining⁴⁰. Adjuvant therapies such as Radiotherapy (RT) and chemotherapy are often used to decrease the risk of recurrence in patients with NPC, however, the survival outcomes remain poor^{41,42}. Our previous study found that resveratrol, a natural product from medicinal herbs had less side effect and can cross blood brain barrier⁴³. It has also been confirmed to exert potential effects against head and neck cancer such as NPC⁴⁴. However, no systematic study of its pharmacological action has been undertaken yet⁴⁵. Recent developments in networks have provided new sight to treat the complex

diseases with bioactive compounds⁴⁶. In order to clarify this issue further, it is necessary to conduct network prediction analysis to explore possible mechanisms underlying resveratrol pharmacological effects on NPC.

In this study, we first evaluated the PK properties and toxicity of resveratrol in human beings to identify guidelines on its application. According to Lipinski's "rule of 5"⁴⁷, the main drug properties were determined with the compounds ranging from 180 to 500 Dalton. In addition, numbers of possible hydrogen-bond donors and acceptors were less than 5 and 10 coupled with a log P value was less than 5⁴⁸. As a result, resveratrol can be satisfied with these standards, which means it could be chosen as an optional compound. As a result, network pharmacological showed that resveratrol was a multitarget drug for NPC treatment. 223 effective NPC targets of resveratrol were presented from the "drug-disease" category through the network pharmacology method for further enrichment analysis. The GO and KEGG results showed that resveratrol generally exerted anti-NPC effects mainly on the factor of kinase binding, transcription factor binding and cytokine receptor binding. The primary pharmacological pathways included PI3K-Akt signaling pathway, apoptosis, MAPK signaling pathway and P53 signaling pathway, etc. The key target of MAPK pathway such as MAPK1, MAPK3, and MAPK8 were mainly reflected in the functions of hub nodes in the network and was further determined in the apoptotic mechanism. Here, network pharmacology and molecular docking provided a theoretical basis for the further verification experiments in NPC pharmacological target and discussion of the mechanisms of resveratrol in the treatment of this disease.

To further clarify the anti-NPC targets of resveratrol, the sensitivity of CNE2 cells was identified after resveratrol treatment. According to our observations, CNE2 cells showed growth arrest and cell shrinkage under 50 μ M and 100 μ M resveratrol treatment for 24 and 48-hour. More than that, TUNEL staining showed that resveratrol exerted the inhibitory effects on apoptosis in CNE2 cells. The wound scratch test and transwell experiments revealed that the capacity of migration and invasion in CNE2 cells was also inhibited with the resveratrol treatment. The above results suggested that CNE cells were sensitive to resveratrol via cellular inhibition and apoptosis induction.

MAPK signaling pathway, which consists of ERK1/2, P38 and JNK was critically involved in many important cellular processes^{49,50}. Its dysregulation led to uncontrolled cellular proliferation, survival, dedifferentiation and anti-apoptotic consequences⁵¹. Several lines of evidence indicated that mutations of MAPK affected development and progression of head and neck squamous cell carcinoma^{52,53}. This further implied that MAPK signaling pathway could be a valuable target for tumor therapy. Here, Western Blot results confirmed that the ratio of phosphorylated ERK1/2 (p-ERK1/2) to total extracellular signal-regulated kinases (ERK1/2) was significantly decreased after 100 μ M resveratrol treatment for 48 hours compared to the control group. Moreover, the expression of p-JNK/JNK and p-P38/P38 in the MAPK pathway was down-regulated simultaneously after resveratrol in time and dose treatment. These findings indicated that resveratrol promoted apoptosis of CNE2 cells through inhibition of the activation of MAPK pathway. To determine whether the activation of MAPK pathway observed in CNE2 cells was also present

in vivo, tissue-based IHC staining was evaluated to profile the expression of the phosphorylation targets in NPC as well as their noncancerous counterparts. As tumor surrounding tissues expressed low levels of p-ERK1/2, p-JNK and p-P38, they were used as the baseline control to evaluate the activation of MAPK pathway in tumor tissues. It was observed that the frequencies of p-ERK1/2 were increased significantly in NPC tissues. Similar trends were also found for p-JNK and p-P38. According to the above notions, MAPK pathway activation implicated that resveratrol might be regarded as a favorable factor of cancer therapy in clinic.

In conclusion, based on network pharmacological analysis, molecular docking and experiment verification in vitro, we believed that the underlying reasons of resveratrol sensitive to NPC cells were associated with MAPK regulated apoptosis signaling pathways. Differential MAPK phosphorylation in NPC patients may indicate sensitive responses of that type of tumor to resveratrol therapy. In the following context, the manipulation of CNE2 cells with suitable MAPK pathway inhibitor might further strengthen this statement.

Declarations

Authors contributions

Bo Zhou and Zihan Xu wrote the original manuscript; Bo Zhou collated the network pharmacology and molecular docking database; Tengjun Man analyzed the cell experimental data and explained the results; Yujuan Yi and Hong Tang performed the data analysis; Zheng Sun supervised and directed the research; Jia Li improved the manuscript; All authors reviewed the manuscript and approved the final version of the manuscript.

Acknowledgment

Thanks to Yang Yu (Foreign Language Department in Dalian Medical University) for editing this English text of a draft of this manuscript.

Funding

This study was supported by the National Natural Science Foundation of China (No. 81702485), the project of Dalian Young Star on Science and Technology (No. 2018RQ64), the Education fund item of Liaoning Province (NO. LJKZ0845) and Foundation of the First Affiliated Hospital of Dalian Medical University (NO. LQ2018D012).

Data availability

All the data shown in this manuscript can be obtained from the open-source website.

Competing interest

We have no conflict of competing interest.

References

1. Wang, Y. et al. Therapeutic target database 2020: enriched resource for facilitating research and early development of targeted therapeutics. *Nucleic Acids Res* 48, D1031-D1041, doi:10.1093/nar/gkz981 (2020).
2. Zeng, X., Liu, G., Pan, Y. & Li, Y. Prognostic Value of Clinical Biochemistry-Based Indexes in Nasopharyngeal Carcinoma. *Front Oncol* 10, 146, doi:10.3389/fonc.2020.00146 (2020).
3. Chen, H. et al. Synthesis and biological evaluation of novel N-(piperazin-1-yl) alkyl-1H-dibenzo [a,c]carbazole derivatives of dehydroabiatic acid as potential MEK inhibitors. *J Enzyme Inhib Med Chem* 34, 1544–1561, doi:10.1080/14756366.2019.1655407 (2019).
4. Shebl, F. M., Bhatia, K. & Engels, E. A. Salivary gland and nasopharyngeal cancers in individuals with acquired immunodeficiency syndrome in United States. *Int J Cancer* 126, 2503–2508, doi:10.1002/ijc.24930 (2010).
5. Ni, H. et al. Inactivation of MSH3 by promoter methylation correlates with primary tumor stage in nasopharyngeal carcinoma. *Int J Mol Med* 40, 673–678, doi:10.3892/ijmm.2017.3044 (2017).
6. Guo, X., O'Brien, S. J., Zeng, Y., Nelson, G. W. & Winkler, C. A. GSTM1 and GSTT1 gene deletions and the risk for nasopharyngeal carcinoma in Han Chinese. *Cancer Epidemiol Biomarkers Prev* 17, 1760–1763, doi:10.1158/1055-9965.EPI-08-0149 (2008).
7. Chow, L. Q. M. et al. Antitumor Activity of Pembrolizumab in Biomarker-Unselected Patients With Recurrent and/or Metastatic Head and Neck Squamous Cell Carcinoma: Results From the Phase Ib KEYNOTE-012 Expansion Cohort. *J Clin Oncol* 34, 3838–3845, doi:10.1200/JCO.2016.68.1478 (2016).
8. Toumi, N., Ennouri, S., Charfeddine, I., Daoud, J. & Khanfir, A. Prognostic factors in metastatic nasopharyngeal carcinoma. *Braz J Otorhinolaryngol*, doi:10.1016/j.bjorl.2020.05.022 (2020).
9. Zhai, S., Huang, Q., Liao, X. & Yin, S. Study on the Drug Targets and Molecular Mechanisms of *Rhizoma Curcumae* in the Treatment of Nasopharyngeal Carcinoma Based on Network Pharmacology. *Evid Based Complement Alternat Med* 2020, 2606402, doi:10.1155/2020/2606402 (2020).
10. Mai, J. et al. Polo-Like Kinase 1 phosphorylates and stabilizes KLF4 to promote tumorigenesis in nasopharyngeal carcinoma. *Theranostics* 9, 3541–3554, doi:10.7150/thno.32908 (2019).
11. Zheng, L. S. et al. SPINK6 Promotes Metastasis of Nasopharyngeal Carcinoma via Binding and Activation of Epithelial Growth Factor Receptor. *Cancer Res* 77, 579–589, doi:10.1158/0008-5472.CAN-16-1281 (2017).
12. Tian, R. et al. Unlocking the Secrets of Mitochondria in the Cardiovascular System: Path to a Cure in Heart Failure-A Report from the 2018 National Heart, Lung, and Blood Institute Workshop. *Circulation* 140, 1205–1216, doi:10.1161/CIRCULATIONAHA.119.040551 (2019).
13. Zhao, H., Zhang, Y., Shu, L., Song, G. & Ma, H. Resveratrol reduces liver endoplasmic reticulum stress and improves insulin sensitivity in vivo and in vitro. *Drug Des Devel Ther* 13, 1473–1485,

- doi:10.2147/DDDT.S203833 (2019).
14. Shaito, A. et al. Potential Adverse Effects of Resveratrol: A Literature Review. *Int J Mol Sci* 21, doi:10.3390/ijms21062084 (2020).
 15. Tian, B. & Liu, J. Resveratrol: a review of plant sources, synthesis, stability, modification and food application. *J Sci Food Agric* 100, 1392–1404, doi:10.1002/jsfa.10152 (2020).
 16. Huang, T. T. et al. Resveratrol induces apoptosis of human nasopharyngeal carcinoma cells via activation of multiple apoptotic pathways. *J Cell Physiol* 226, 720–728, doi:10.1002/jcp.22391 (2011).
 17. Oi, N. et al. Resveratrol, a red wine polyphenol, suppresses pancreatic cancer by inhibiting leukotriene A(4) hydrolase. *Cancer Res* 70, 9755–9764, doi:10.1158/0008-5472.CAN-10-2858 (2010).
 18. Zhang, M., Zhou, X. & Zhou, K. Resveratrol inhibits human nasopharyngeal carcinoma cell growth via blocking pAkt/p70S6K signaling pathways. *Int J Mol Med* 31, 621–627, doi:10.3892/ijmm.2013.1237 (2013).
 19. Deng, Y. et al. Integrated Phytochemical Analysis Based on UPLC-Q-TOF-MS/MS, Network Pharmacology, and Experiment Verification to Explore the Potential Mechanism of *Platycodon grandiflorum* for Chronic Bronchitis. *Front Pharmacol* 11, 564131, doi:10.3389/fphar.2020.564131(2020).
 20. Liu, T. H. et al. Verification of Resveratrol Inhibits Intestinal Aging by Downregulating ATF4/Chop/Bcl-2/Bax Signaling Pathway: Based on Network Pharmacology and Animal Experiment. *Front Pharmacol* 11, 1064, doi:10.3389/fphar.2020.01064 (2020).
 21. Yang, F. et al. The Interventional Effects of Tubson-2 Decoction on Ovariectomized Rats as Determined by a Combination of Network Pharmacology and Metabolomics. *Front Pharmacol* 11, 581991, doi:10.3389/fphar.2020.581991 (2020).
 22. Wang, W. et al. Resveratrol: Multi-Targets Mechanism on Neurodegenerative Diseases Based on Network Pharmacology. *Front Pharmacol* 11, 694, doi:10.3389/fphar.2020.00694 (2020).
 23. Ru, J. et al. TCMSP: a database of systems pharmacology for drug discovery from herbal medicines. *J Cheminform* 6, 13, doi:10.1186/1758-2946-6-13 (2014).
 24. Yi, F. et al. In silico Approach for Anti-Thrombosis Drug Discovery: P2Y1R Structure-Based TCMS Screening. *Front Pharmacol* 7, 531, doi:10.3389/fphar.2016.00531 (2016).
 25. Kim, S. et al. PubChem in 2021: new data content and improved web interfaces. *Nucleic Acids Res* 49, D1388-D1395, doi:10.1093/nar/gkaa971 (2021).
 26. Daina, A., Michielin, O. & Zoete, V. SwissTargetPrediction: updated data and new features for efficient prediction of protein targets of small molecules. *Nucleic Acids Res* 47, W357-W364, doi:10.1093/nar/gkz382 (2019).
 27. Wishart, D. S. et al. DrugBank 5.0: a major update to the DrugBank database for 2018. *Nucleic Acids Res* 46, D1074-D1082, doi:10.1093/nar/gkx1037 (2018).

28. Wang, X. et al. PharmMapper 2017 update: a web server for potential drug target identification with a comprehensive target pharmacophore database. *Nucleic Acids Res* 45, W356-W360, doi:10.1093/nar/gkx374 (2017).
29. Gfeller, D. et al. SwissTargetPrediction: a web server for target prediction of bioactive small molecules. *Nucleic Acids Res* 42, W32-38, doi:10.1093/nar/gku293 (2014).
30. McGarvey, P. B. et al. UniProt genomic mapping for deciphering functional effects of missense variants. *Hum Mutat* 40, 694–705, doi:10.1002/humu.23738 (2019).
31. Pinero, J. et al. The DisGeNET knowledge platform for disease genomics: 2019 update. *Nucleic Acids Res* 48, D845-D855, doi:10.1093/nar/gkz1021 (2020).
32. Fishilevich, S. et al. Genic insights from integrated human proteomics in GeneCards. Database (Oxford) 2016, doi:10.1093/database/baw030 (2016).
33. Wang, G. N. et al. O Blood Type Is Associated with Unfavorable Distant-metastasis-free Survival in Female Patients with Nasopharyngeal Carcinoma: A Retrospective Study of 2439 Patients from Epidemic Area. *J Cancer* 10, 1297–1306, doi:10.7150/jca.28372 (2019).
34. Amberger, J. S., Bocchini, C. A., Schiettecatte, F., Scott, A. F. & Hamosh, A. OMIM.org: Online Mendelian Inheritance in Man (OMIM(R)), an online catalog of human genes and genetic disorders. *Nucleic Acids Res* 43, D789-798, doi:10.1093/nar/gku1205 (2015).
35. Davis, A. P. et al. Comparative Toxicogenomics Database (CTD): update 2021. *Nucleic Acids Res* 49, D1138-D1143, doi:10.1093/nar/gkaa891 (2021).
36. Demchak, B. et al. Cytoscape: the network visualization tool for GenomeSpace workflows. *F1000Res* 3, 151, doi:10.12688/f1000research.4492.2 (2014).
37. Burley, S. K. Impact of structural biologists and the Protein Data Bank on small-molecule drug discovery and development. *J Biol Chem* 296, 100559, doi:10.1016/j.jbc.2021.100559 (2021).
38. Gu, M. et al. PFKFB3 promotes proliferation, migration and angiogenesis in nasopharyngeal carcinoma. *J Cancer* 8, 3887–3896, doi:10.7150/jca.19112 (2017).
39. Zhuang, M. et al. Effusanin E suppresses nasopharyngeal carcinoma cell growth by inhibiting NF-kappaB and COX-2 signaling. *PLoS One* 9, e109951, doi:10.1371/journal.pone.0109951 (2014).
40. Zhao, Y. et al. High expression of Sox10 correlates with tumor aggressiveness and poor prognosis in human nasopharyngeal carcinoma. *Onco Targets Ther* 9, 1671–1677, doi:10.2147/OTT.S101344 (2016).
41. Li, Q. J. et al. A Nomogram Based on Serum Biomarkers and Clinical Characteristics to Predict Survival in Patients with Non-Metastatic Nasopharyngeal Carcinoma. *Front Oncol* 10, 594363, doi:10.3389/fonc.2020.594363 (2020).
42. Li, Y. et al. EZH2-DNMT1-mediated epigenetic silencing of miR-142-3p promotes metastasis through targeting ZEB2 in nasopharyngeal carcinoma. *Cell Death Differ* 26, 1089–1106, doi:10.1038/s41418-018-0208-2 (2019).

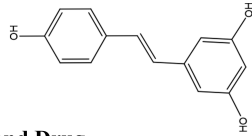
43. Sun, Z. et al. Evaluation of resveratrol sensitivities and metabolic patterns in human and rat glioblastoma cells. *Cancer Chemother Pharmacol* 72, 965–973, doi:10.1007/s00280-013-2274-y (2013).
44. Kong, J. & Wang, W. A Systemic Review on the Regulatory Roles of miR-34a in Gastrointestinal Cancer. *Onco Targets Ther* 13, 2855–2872, doi:10.2147/OTT.S234549 (2020).
45. Strotskaya, A. et al. The action of Escherichia coli CRISPR-Cas system on lytic bacteriophages with different lifestyles and development strategies. *Nucleic Acids Res* 45, 1946–1957, doi:10.1093/nar/gkx042 (2017).
46. Ong, M. S. et al. Learning a Comorbidity-Driven Taxonomy of Pediatric Pulmonary Hypertension. *Circ Res* 121, 341–353, doi:10.1161/CIRCRESAHA.117.310804 (2017).
47. Saxena, R. et al. Preclinical Development of a Nontoxic Oral Formulation of Monoethanolamine, a Lipid Precursor, for Prostate Cancer Treatment. *Clin Cancer Res* 23, 3781–3793, doi:10.1158/1078-0432.CCR-16-1716 (2017).
48. Mugumbate, G. & Overington, J. P. The relationship between target-class and the physicochemical properties of antibacterial drugs. *Bioorg Med Chem* 23, 5218–5224, doi:10.1016/j.bmc.2015.04.063 (2015).
49. Fedele, C. et al. SHP2 Inhibition Prevents Adaptive Resistance to MEK Inhibitors in Multiple Cancer Models. *Cancer Discov* 8, 1237–1249, doi:10.1158/2159-8290.CD-18-0444 (2018).
50. Gonzalez-Teran, B. et al. p38gamma and delta promote heart hypertrophy by targeting the mTOR-inhibitory protein DEPTOR for degradation. *Nat Commun* 7, 10477, doi:10.1038/ncomms10477 (2016).
51. Yaeger, R. & Corcoran, R. B. Targeting Alterations in the RAF-MEK Pathway. *Cancer Discov* 9, 329–341, doi:10.1158/2159-8290.CD-18-1321 (2019).
52. Kasitinon, S. Y. et al. TRPML1 Promotes Protein Homeostasis in Melanoma Cells by Negatively Regulating MAPK and mTORC1 Signaling. *Cell Rep* 28, 2293–2305 e2299, doi:10.1016/j.celrep.2019.07.086 (2019).
53. Ngan, H. L. et al. MAPK pathway mutations in head and neck cancer affect immune microenvironments and ErbB3 signaling. *Life Sci Alliance* 3, doi:10.26508/lsa.201900545 (2020).

Figures

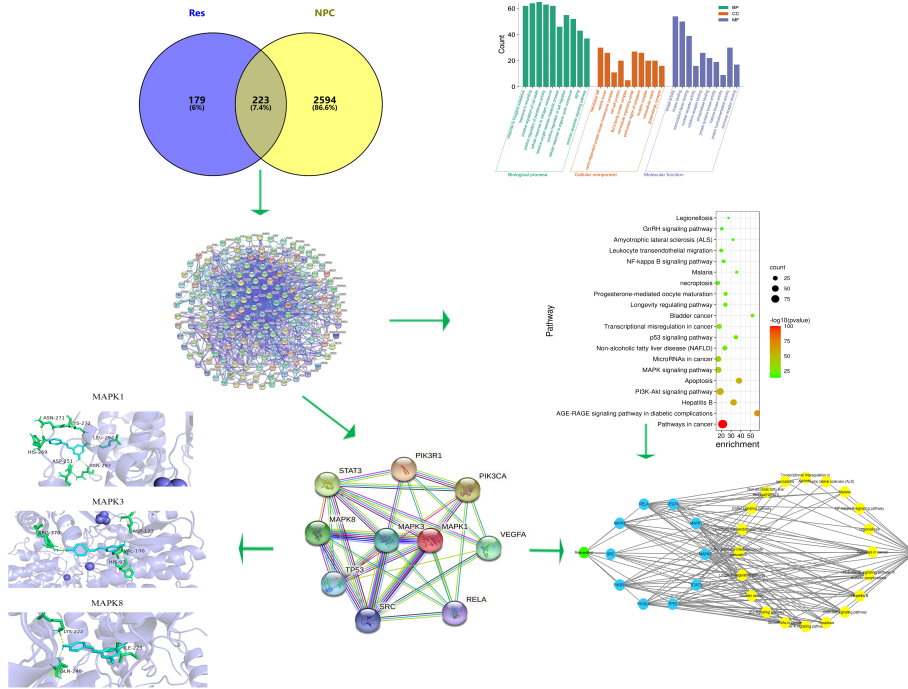
Nasopharyngeal carcinoma



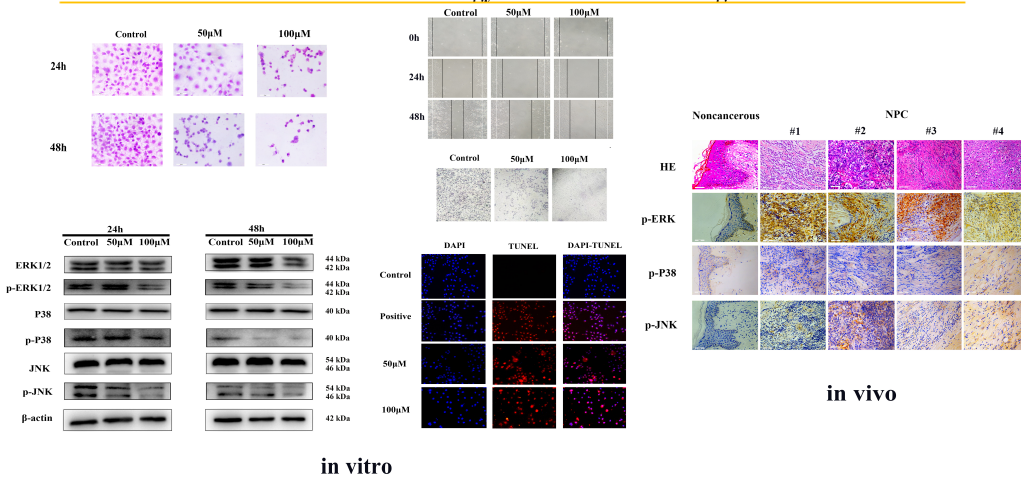
Resveratrol



Disease and Drug



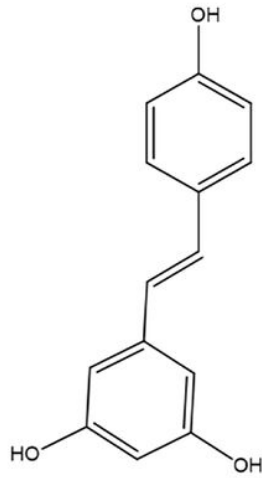
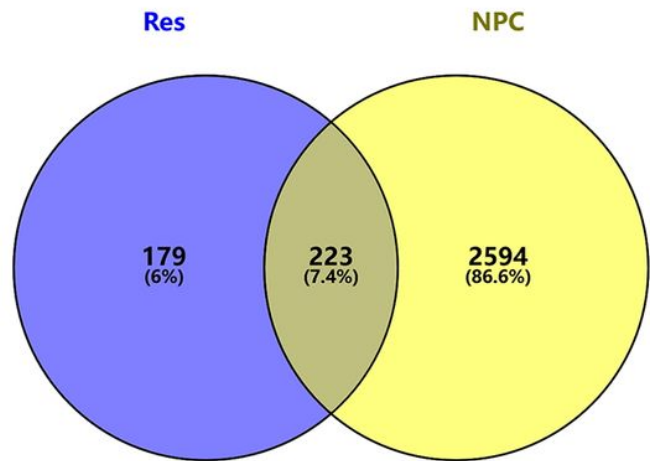
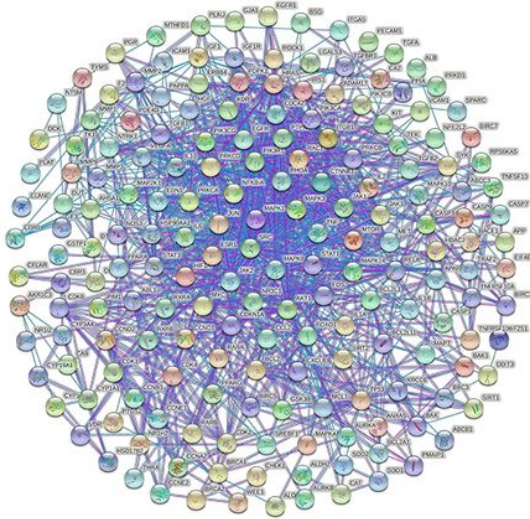
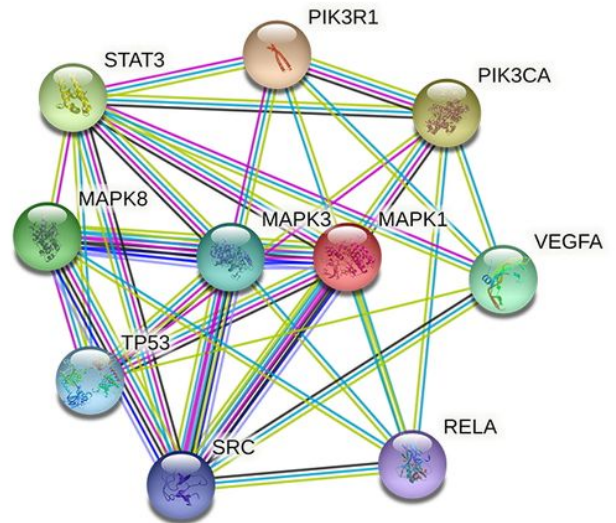
Network Pharmacology and Molecular docking



Experimental validation

Figure 1

Graphical abstract

A**B****C****D****Figure 2**

(A) Chemical structure of resveratrol. (B) Venn diagram of intersecting targets. (C) PPI network in NPC with resveratrol treatment. (D) Predictive patterns of 10 hub genes.

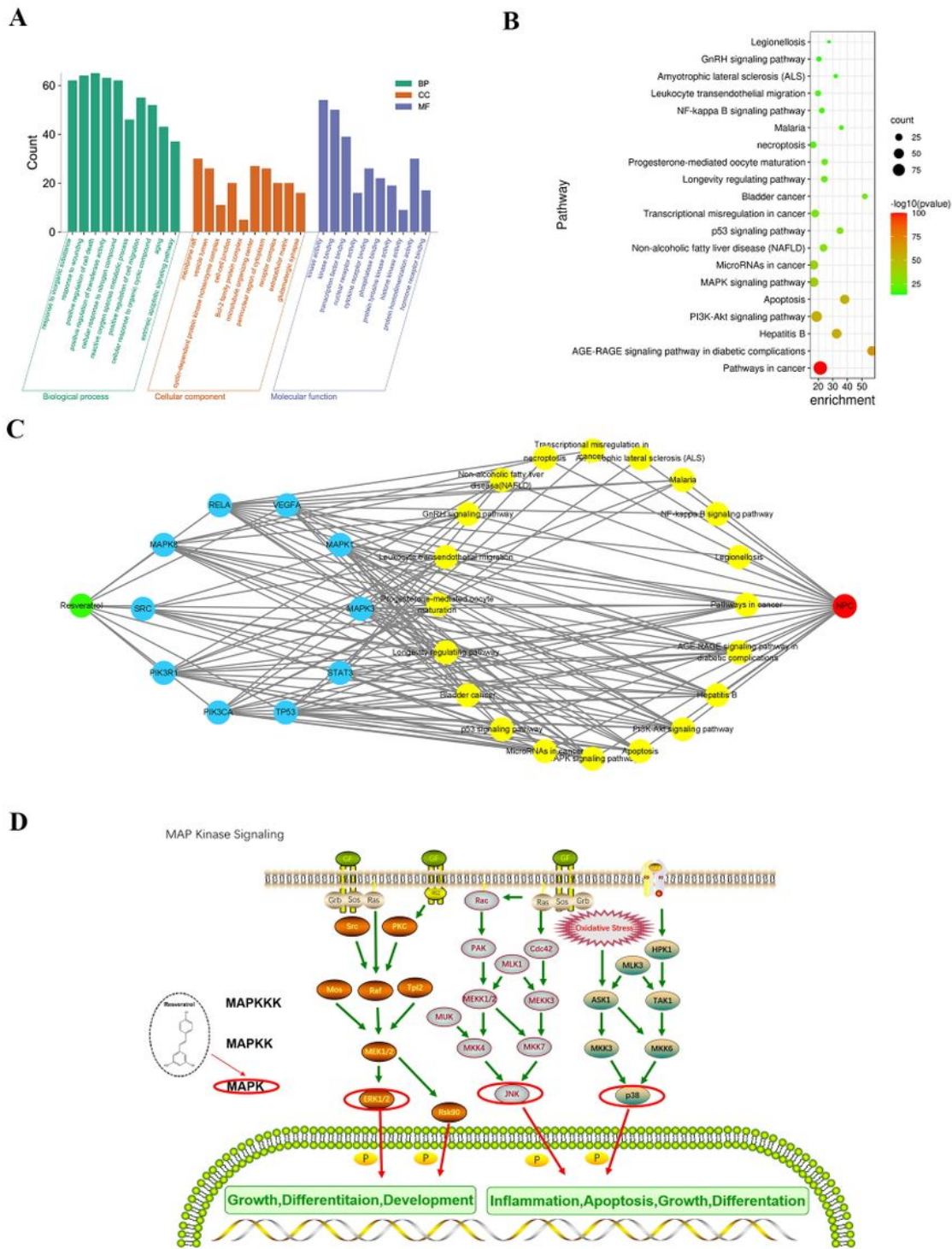


Figure 3

(A) GO enrichment analysis. (B) The enrichment of top 20 pathways on target genes. (C) Component-target-disease-pathway interaction network. (D) Resveratrol inhibited the development of NPC by regulating the MAPK signal pathway.

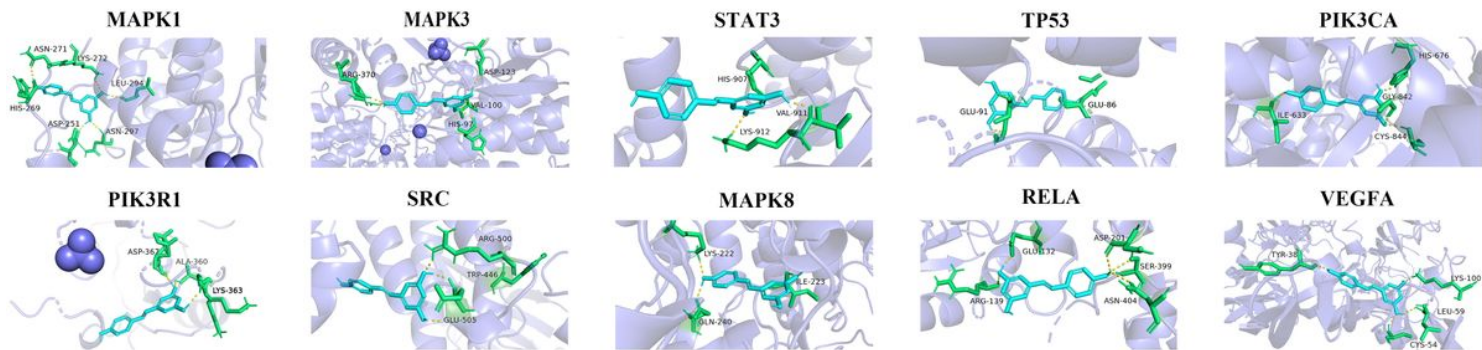
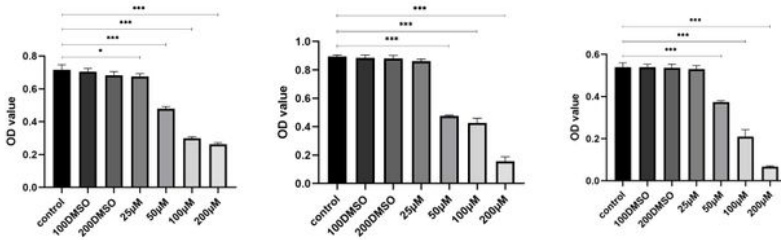


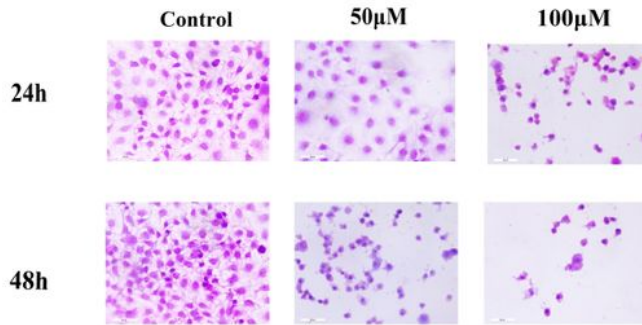
Figure 4

Theoretical studies on the structural interactions of key targeting receptors for resveratrol.

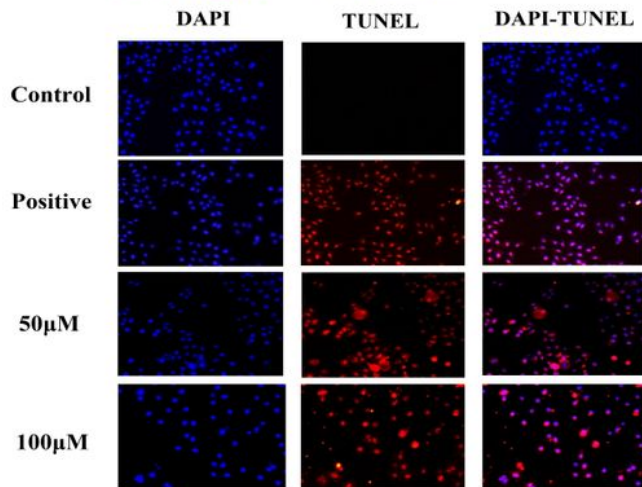
A



B



C



D

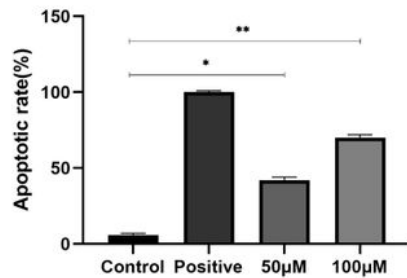


Figure 5

Effects of 50 and 100 mM resveratrol treatment on NPC CNE2 cell line. (A) CCK8 assay was used to detect the proliferation of CNE2 cells with resveratrol treatment for 24, 48 and 72 hours. (B) HE staining method was utilized to notice the morphological and quantitative changes of CNE2 cells treated with resveratrol. (C) The apoptosis-positive cells of CNE2 cells were detected after resveratrol treatment at 50

and 100 mM for 48 hours by TUNEL staining ($\times 100$ magnification). (D) Quantification of CNE2 cell apoptosis. Statistical significance was determined by $*P < 0.05$; $**P < 0.01$; $***P < 0.001$.

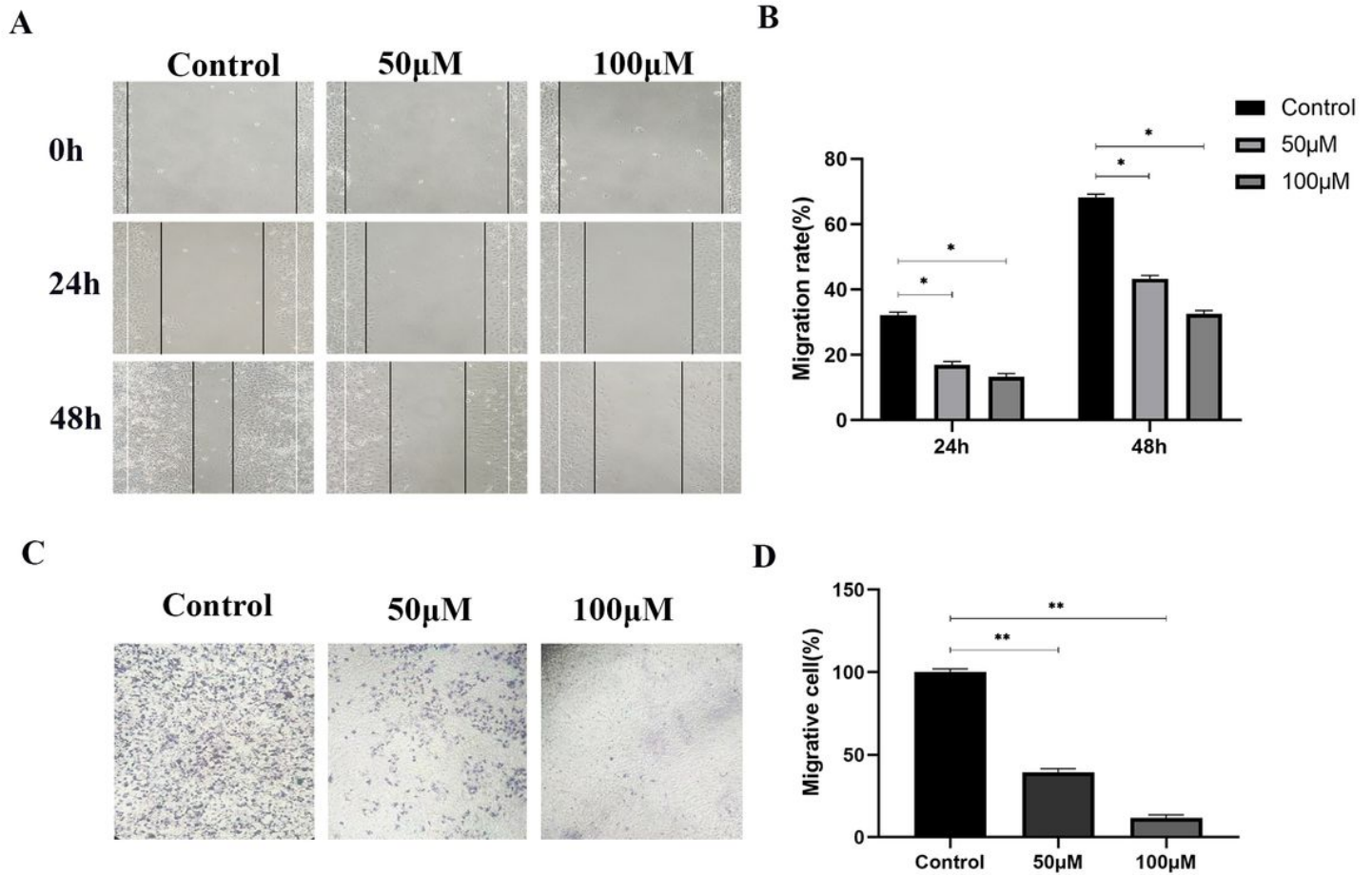


Figure 6

(A) The changes of migration capacity in CNE2 cells treated with Resveratrol at 0, 24 and 48 hours by the wound-healing assay. (B) Migration index analysis of CNE2 cells treated with Resveratrol. (C) Representative images of the CNE2 cells treated with Resveratrol by transwell. (D) Histograms showed the percentage of migrating cells. Data were shown as mean \pm SD. Statistical significance was noted by $*P < 0.05$; $**P < 0.01$.

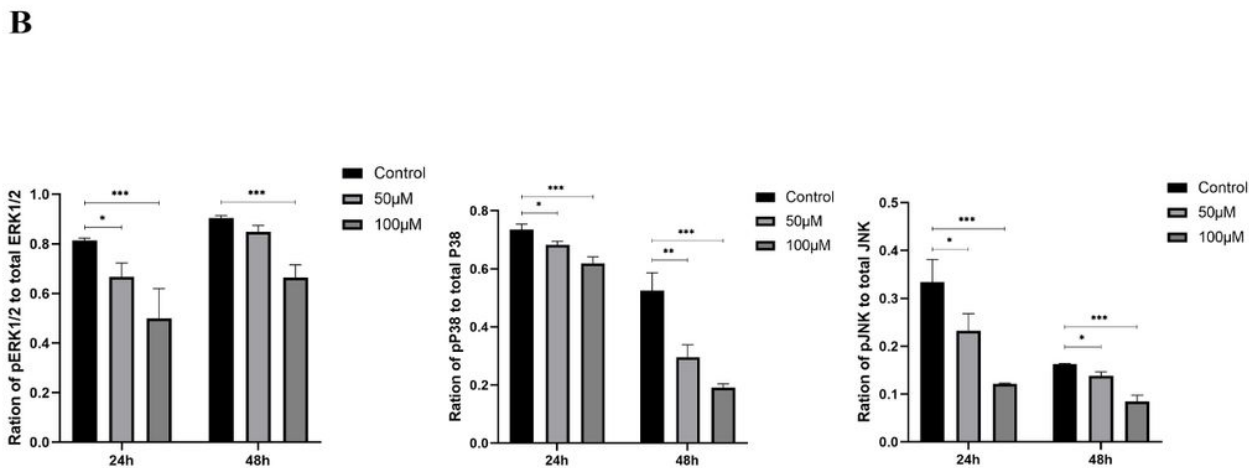
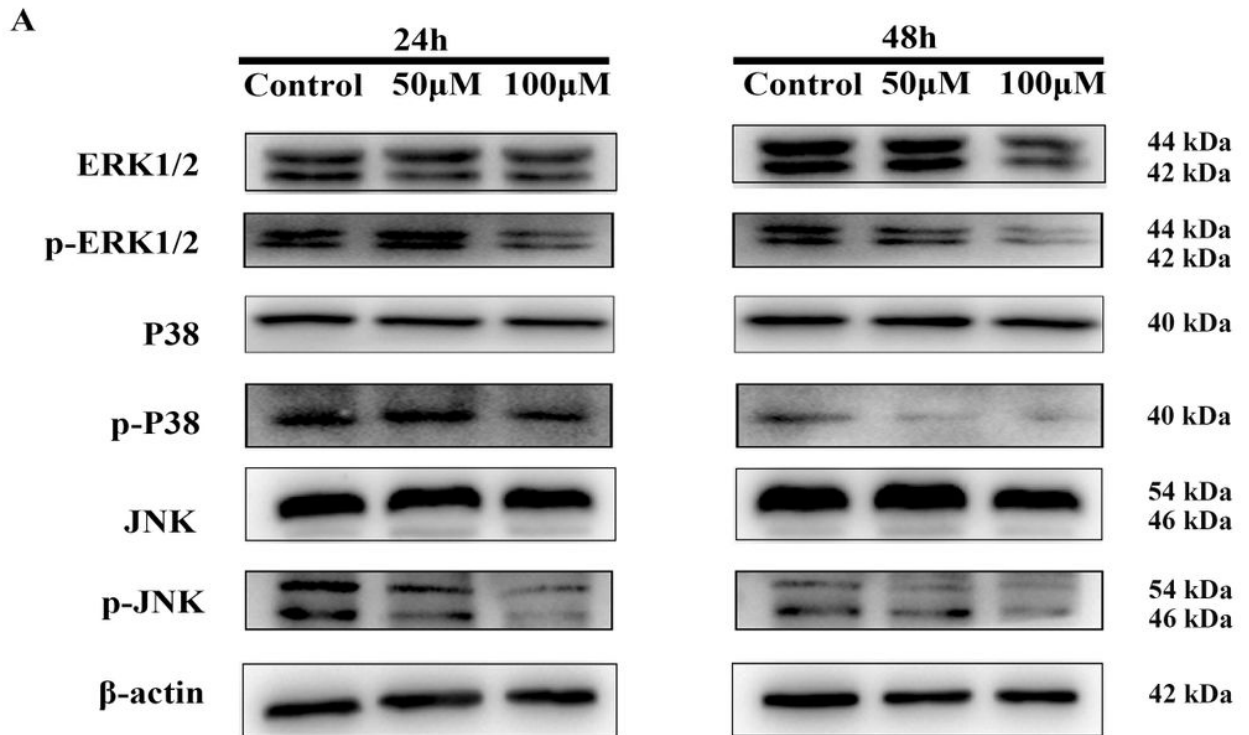


Figure 7

Resveratrol inhibited the activation of MAPK signaling pathway. (A) Effects of Resveratrol on ERK1/2, p-ERK1/2, JNK, p-JNK, P38 and p-P38 protein levels in CNE2 cells in view of the Western Blotting measure; (B) Statistical analysis affecting the ratio of phosphorylated protein to total protein. Data were shown as mean \pm SD. Statistical significance was determined by * P <0.05, ** P <0.01 and *** P <0.001.

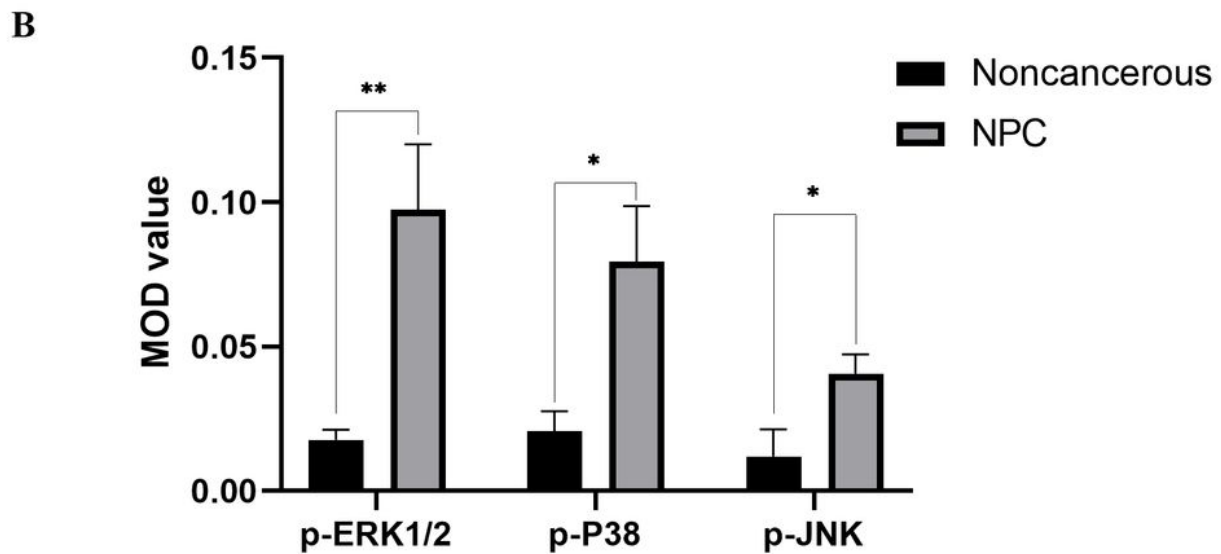
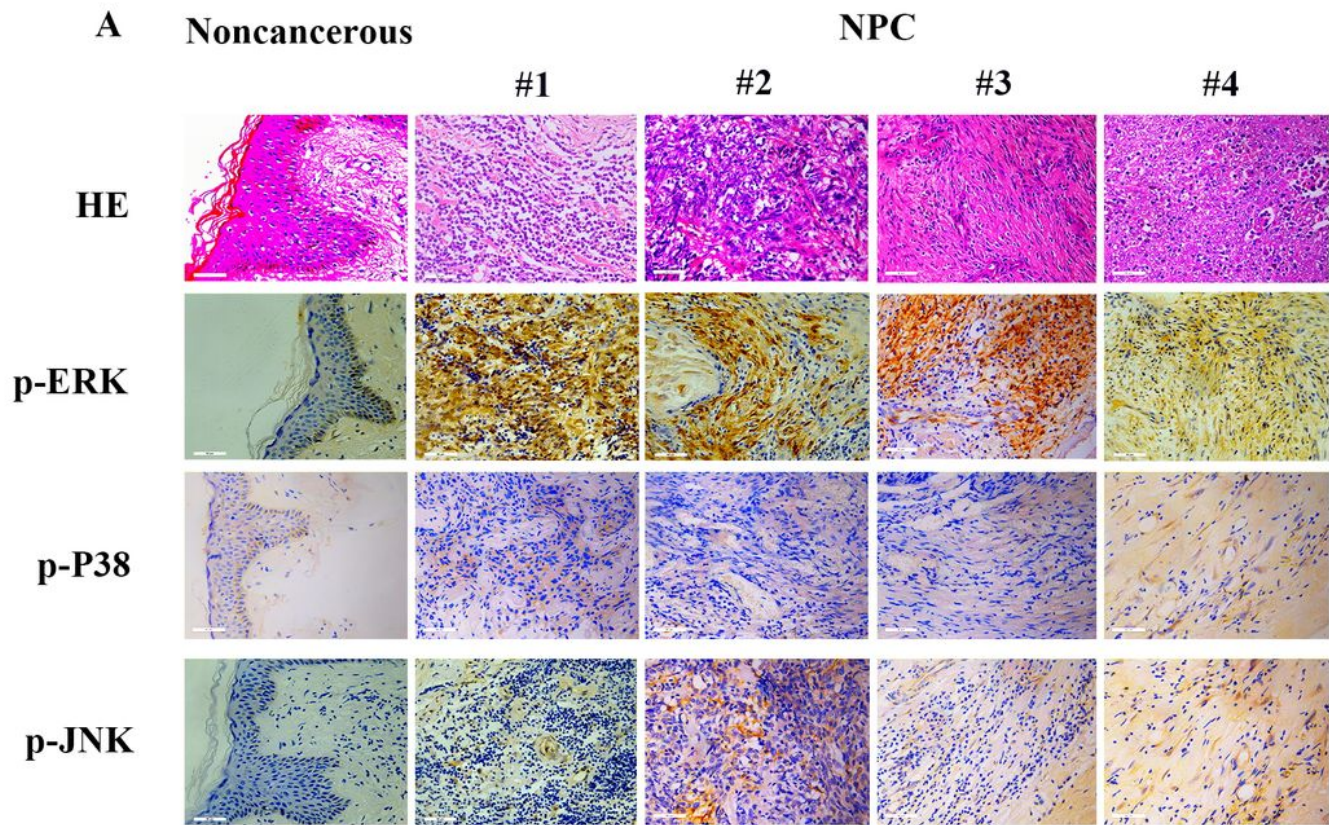


Figure 8

Immunohistochemistry images of p-ERK1/2, p-P38 and p-JNK in NPC tissues and noncancerous tissues of patients in different cases. Micrographs of IHC staining (segments in first line were counterstained with hematoxylin eosin; $\times 400$ magnification), and their investigations showed the declaration expression of p-ERK1/2, p-P38 and p-JNK. MOD signified the mean optical density of the areas. $*P < 0.05$ or $**P < 0.01$ versus the control group.

Supplementary Files

This is a list of supplementary files associated with this preprint. Click to download.

- [newSupplementaryTable1.pdf](#)
- [newSupplementaryTable2.pdf](#)
- [newSupplementaryTable3.pdf](#)
- [newSupplementaryTable4.pdf](#)
- [supplementarydataMAPKpathway.zip](#)